POLYMERS FOR ADVANCED TECHNOLOGIES
Polym. Adv. Technol. **11**, 617–625 (2000)

Pore Structure of Superporous Hydrogels

Richard A. Gemeinhart†, Haesun Park and Kinam Park*
Purdue University, Departments of Pharmaceutics and Biomedical Engineering, West Lafayette, IN 47907-1336

ABSTRACT

Hydrogels with a fast swelling property have been synthesized using a gas blowing technique. Since those hydrogels possess interconnected pores of which diameters are in the order of a few hundred micrometers, they are called "superporous hydrogels" (SPHs). The fast swelling of SPHs in aqueous solution is due to the absorption of water by capillary pressure through interconnected pores (i.e. open channels). Because of the importance of pore structures on the fast swelling property, effects of surface porosity on the swelling kinetics were examined. The surface chemistry of the polymerization mold made of glass was varied using various silanes, and the surface morphology of the synthesized SPHs was examined by scanning electron microscopy. The porosity was measured using mercury porosimetry. Despite differences in surface morphology and surface porosity of SPHs, the swelling kinetics were not changed significantly. The internal pore structures remained the same as the surface porosity changed. The study indicates that the swelling of SPHs is predominantly determined by the internal pore structures, and small differences in the surface porosity do not alter the overall swelling kinetics of SPHs. Copyright © 2000 John Wiley & Sons, Ltd.

KEYWORDS: hydrogels; pore structure; superporous hydrogel; foam; superabsorbent; silanes

* Correspondence to: Kinam Park, Purdue University, School of Pharmacy, West Lafayette, IN 47907-1336, USA. E-mail: park@purdue.edu
† Current address: Cornell University, School of Chemical Engineering, Ithaca, NY 14853-5201, USA.
This paper was presented at PAT'99 – Tokyo.

INTRODUCTION

Since the first paper on hydrogels by Wichterle and Lim [1], hydrogels have been used widely in various pharmaceutical and biomedical applications. Controlled drug delivery has been one of the main areas of research utilizing hydrogels. One of the properties of hydrogels, useful in controlled drug delivery, is slow swelling of dry hydrogels in aqueous solution. The slow swelling, which provides a mechanism to control the drug release for long periods of time, is due to absorption of water into the glassy hydrogel by diffusion. While slow swelling of dried hydrogels has been beneficial for many applications, there are situations where fast swelling of dried hydrogels on the order of minutes rather than hours is desirable.

We have been interested in fast swelling hydrogels for development of gastric retention devices [2, 3]. Gastric retention of hydrogels is based on the fast swelling of dried hydrogels to a size larger than the pyloric sphincter. Since the swelling of dried hydrogels is limited by diffusion of water into the hydrogel, the most common method of making fast swelling hydrogels was to reduce the diffusional path length, i.e. to reduce the dimension of the hydrogels. This approach has an obvious limitation of not using hydrogels with dimensions useful in drug delivery. Recently, we synthesized superporous hydrogels (SPHs) that swell in aqueous solution to equilibrium state in a matter of a minute regardless of their size [4]. Such a fast swelling is due to absorption of water by capillary force rather than by simple diffusion. SPHs have interconnected pores forming open channels for capillary absorption of water. Since the pore structure at the surface of hydrogels is thought to be important for fast absorption of water, we investigated pore structures of SPHs in detail.

Received 2 September 1999
Accepted 25 October 1999

SPHs have been made by introducing a gas-forming agent during polymerization. Since the generated gas bubbles rise from the bottom to the top of the polymerization mold, the porous structures are formed longitudinally. Gas bubbles on the surface of the mold are usually trapped against the mold, and this makes little interconnection with the flow of gas evolving from the bottom. The process of foam formation by gas forming agents resulted in oriented pore structures. This study examined the effect of the surface chemistry of the polymerization mold on the pore structure of the SPH surface.

EXPERIMENTAL

Preparation of Superporous Hydrogels

All chemicals were obtained from Aldrich Chemical Company (Milwaukee, WI) and used as received unless otherwise stated. SPHs were produced using acrylic acid and acrylamide with N,N′-methylene-bis-acrylamide (BIS) as the cross-linker in concentrations of 15 (w/v)%, 10 (v/v)%, and 0.25 (w/v)%, respectively. Pluronic® F127 (BASF Corporation, Parsippany, NJ) was added at a concentration of 0.5 (w/v)%. The redox initiator pair, N,N,N′,N′-tetramethylene diamine (TEMED) and ammonium persulfate (APS), were added at a concentration of 2% to the weight of monomer with TEMED being added to the stock monomer solution, and APS being added to the solution at the time of polymerization. Once the stock monomer solution was made, the pH of the solution was adjusted to 5.1 using 50 (w/v)% sodium hydroxide. This solution was added to a 16 mm × 100 mm borosilicate culture tube (Fisher Scientific, Pittsburgh, PA) along with the appropriate amount of APS. Sodium bicarbonate (50 mg, Mallinkrodt Specialty Chemical Co, Paris, KY) was added 210 sec after adding the APS. The tube was mixed thoroughly, after adding sodium bicarbonate, using a spatula to wet the sodium bicarbonate and to distribute the sodium bicarbonate evenly throughout the tube. Polymerization was allowed to proceed for the next 4 hr prior to the addition of absolute ethanol (McCormick Distilling Co., Brookfield, CT). Finally, the SPHs were dried in a food dehydrator (Mr. Coffee, Inc., Bedford Heights, OH) at a temperature of 80°C for 6 hr. For some experiments, conventional hydrogels were produced to determine the difference in properties between SPHs and hydrogels. The same procedures were used to produce the hydrogels, with 20 μl of 50% sodium hydroxide being added instead of 50 mg sodium bicarbonate to mimic the pH change of the solution without having the foam production. Two types of conventional hydrogels were produced: one with the same volume and one with the same mass as the SPHs.

Modification of Glass Tubes with Silanes

To determine the effect of surface chemistry on the surface of the SPHs, borosilicate culture tubes were modified with various silane molecules. The culture tubes were first washed in a chromic acid solution (Fisher) followed by repeated rinsing with deionized distilled water. Glass cover slips (#1 thickness, Bellco Glass Inc., Vineland, NJ) were also modified for determining the air–water–surface contact angle. The cover slips were added to culture tubes and the same procedures were followed as for the culture tubes, with care taken not to touch the cover slips. After washing, the culture tubes were dried in a 70°C oven for at least 12 hr. All glass was used immediately upon removal from the oven. Dimethyl dichlorosilane (DDS), n-butyl trichlorosilane (BTS), n-octyl trichlorosilane (OTS), n-dodecyl trichlorosilane (DTS), n-hexadecyl trichlorsilane (HDTS), n-octadecyl trichlorosilane (ODTS), 2-(carboxymethoxy) ethyl trichlorosilane (CETS), bis(2-hydroxyethyl)-3-aminopropyl triethoxysilane (HATS), n-trimethoxy silyl propyl ethylene diamine triacetic acid (TATS), and 3-aminopropyl triethoxysilane (APTS) were all obtained from United Chemical Technologies (Bristol, PA). Of these chemicals, DDS, BTS, OTS, DTS, HDTS, OTS, and CETS were mixed with methylene chloride to make 2 (v/v)% solutions while HATS, TATS, and APTS were mixed 2 (v/v)% with a 95 (v/v)% ethanol solution made with water and adjusted to a pH of 4.5 using acetic acid. The solution was added to the culture tubes and allowed to react for 3–4 hr. After the reaction was complete, the solutions were discarded individually and the culture tubes rinsed twice with methylene chloride and once with ethanol. Those reacted in ethanol were washed three times with ethanol.

The reaction of the silanes with glass surfaces was examined using contact angle measurement. The glass cover slip was placed in a chamber saturated with deionized water. To the cover slip, 5 μl of deionized water was added and allowed to equilibrate. The air–water–surface contact angles were measured using a goniometer (Ramé-Hart Inc., Mountain Lake, NJ). After the advancing contact angle was obtained, an additional 20 μl of deionized water was added and allowed to equilibrate. The 20 μl was removed with a microsyringe, and the receding angle was measured. Four measurements were taken on each cover slip for both the advancing and receding contact angles, and three independent cover slips were examined.

Mercury Porosimetry

Pore sizes of SPHs were determined using a mercury porosimeter (Autopore II 9220, Micromeritics, Norcross, GA). A 6 ml penetrometer was used for all experiments. The compressibility of the mercury, sample, and penetrometer were accounted for using standard procedures. Samples were taken from the 80°C oven and cut into 1 cm sections. Three samples from one SPH were considered a single data point. This was done due to the large pore volume of the sample. Since a pore

volume of 0.38 ml was the maximum intrusion volume that could be measured, it was necessary to reduce the size of each piece. Three groups of the three measurements were examined for each sample.

Samples were examined using two pressure regimens. The first pressure regimen was used for initial samples and to confirm the lack of pores outside the range chosen for the second regimen. This regimen utilized the standard pressures that are used to examine various samples, such as tablets and concrete. The second pressure regimen was used for all SPHs. It used more points at lower pressure to more closely examine the exact pore size. Data was analyzed using the Laplace equation [5] which is shown in eq. (1) after correction for compressibility of mercury and sample:

$$d = \frac{-4\gamma \cos\theta}{P} \tag{1}$$

From the Laplace equation, the diameter of the pores (d) can be calculated when the contact angle (θ), and the surface tension of the intruding liquid (γ) are known for a given pressure (P). The contact angle was found to be $137.2 \pm 0.6°$ and the surface tension of mercury was 480 dyne/cm. The average pore diameter was determined from the graph of percent maximum intrusion volume v. pore diameter. The diameter at which the intrusion volume is half the maximal value was considered the average diameter.

The density of samples can also be calculated using mercury porosimetry. The samples are surrounded by a non-wetting liquid, mercury. The mass (m) of the sample is known. From the weight of the mercury, the volume of the sample can be calculated prior to intrusion into the pores. The volume ($V_{0.5\text{psia}}$) of the sample is determined at 0.5 psia at which no intrusion will take place. At a pressure of 60,000 psia, all pores are filled with intruding mercury and the volume ($V_{60{,}000\text{psia}}$) of the sample is again determined. The density of the bulk material and the volume of the solid material are calculated from eqs (2) and (3), respectively:

$$\rho_{\text{bulk}} = \frac{m}{V_{0.5\text{psia}}} \tag{2}$$

$$\rho_{\text{solid}} = \frac{m}{V_{60{,}000\text{psia}}} \tag{3}$$

Scanning Electron Microscopy

Scanning electron microscopy (SEM) was used to determine the morphology of the dried samples. A JEOL JSM-840 scanning electron microscope (Jeol USA, Inc., Peabody, MA) was used after coating the samples with gold using a Hummer Sputter Coater (Technics, Ltd.). Images were captured using a digital capture card and Digital Scan Generator 1 (Jeol). Samples were cut using a scalpel to allow for the appropriate portion of the sample to be visible to the SEM. Samples were blown clean using compressed air (Envi-Ro-Tech™ Duster 1671, Tech Spray, Inc., Amarillo, TX), to remove any particles of the broken SPH.

TABLE 1. Advancing and Receding Contact Angles on Modified Glass Surfaces ($n = 3$)

Functional groups	*θa (°)*	*θr (°)*
Glass	49.6 ± 2.1	27.6 ± 5.4
DDS	93.0 ± 2.2	87.8 ± 1.2
BTS	99.2 ± 1.8	80.5 ± 4.7
OTS	101.5 ± 2.0	77.8 ± 2.5
DDTS	105.1 ± 2.7	79.9 ± 1.9
HDTS	104.9 ± 3.0	84.3 ± 1.7
ODTS	102.2 ± 1.7	80.8 ± 3.6
CETS	59.5 ± 2.9	46.8 ± 3.9
BATS	36.3 ± 3.5	21.8 ± 2.8
TATS	24.2 ± 1.7	5.1 ± 1.3
APTES	44.3 ± 7.5	18.3 ± 4.6

Swelling Studies

Swelling experiments were conducted using phosphate buffered saline (PBS; pH 7.4, $I = 0.18$ M). All data was obtained in triplicate. Samples were weighed and added to the PBS. At each time point from 15 sec through 20 min, the sample was removed from the PBS. The sample was blotted with a Kimwipe® (Kimberly-Clark Corp., Roswell, GA) to remove excess water from the surface. Some water was still present in the pore structure, however, this water was difficult to remove without sufficient force and was thus considered part of the SPH. To take into account slight variations in the starting mass, the mass swelling ratio was used to examine the results of the experiment. Equation (4) was used to calculate the mass swelling ratio, q, by using the dry weight, w_d, and the swollen weight, w_s.

$$q = \frac{w_s}{w_d} \tag{4}$$

RESULTS

Surface Morphology

Table 1 contains the silanes that were used for this study and the air–water–surface contact angles measured for individual surfaces. The contact angle of the functionalized surfaces varied greatly from unmodified glass indicating that successful surface functionalization had taken place. It is well accepted that the silanes have high surface coverage [6]. A broad range of surface properties was chosen for this study. As the hydrophobic chain was extended from n-octyl to n-octadecyl, the contact angle varied only slightly indicating that the surface did not become more hydrophobic. Of the hydrophilic surfaces, the TATS surface had the

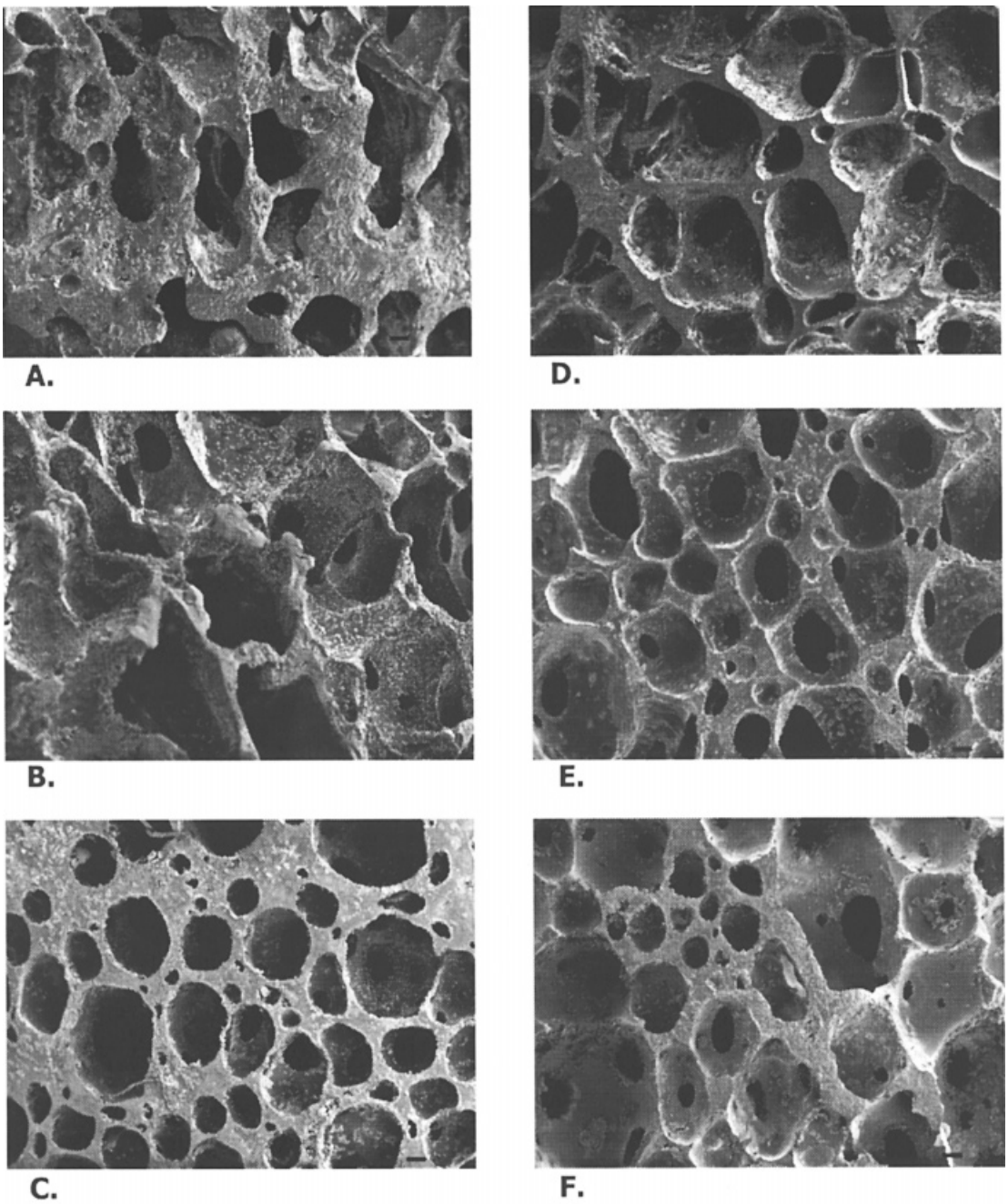

FIGURE 1. Scanning electron micrographs of the surface of poly(acrylamide-co-acrylic acid) superporous hydrogels produced using surfaces modified with hydrophobic agents. The micrographs of the surface of superporous hydrogels produced in glass tubes with DDS (A), BTS (B), OTS (C), DDTS (D), HDTS (E), ODTS (F) surfaces were taken at a magnification of 50× and the scale bar is 100 μm.

lowest contact angle indicating the greatest hydrophilicity.

SPHs produced in culture tubes modified with each of the compounds showed very different surfaces, even to the naked eye. With the exception of the amine functionalized surfaces, the surface of the SPHs were examined using SEM. Two distinct groups were found by comparing the surface structure of the SPHs. Regardless of the functionality (C1–C18), all of the hydrophobic functionalized surfaces produced a porous surface structure (Fig. 1). All surfaces were quite rough with some difference in the apparent roughness between samples. The DDS sample was the most irregular while the ODTS, HDTS, and DDTS were all similar. Regardless of the functionality, all of the hydrophilic surfaces produced relatively non-porous surfaces (Fig. 2). Swelling experiments (Fig. 3) showed that the SPHs produced in hydrophilic modified glass took almost equivalent times to reach equilibrium as those produce with hydrophobic surfaces ($p > 0.10$). It appears that the surface porosity on the side of cylindrical SPHs did not influence the swelling kinetics significantly.

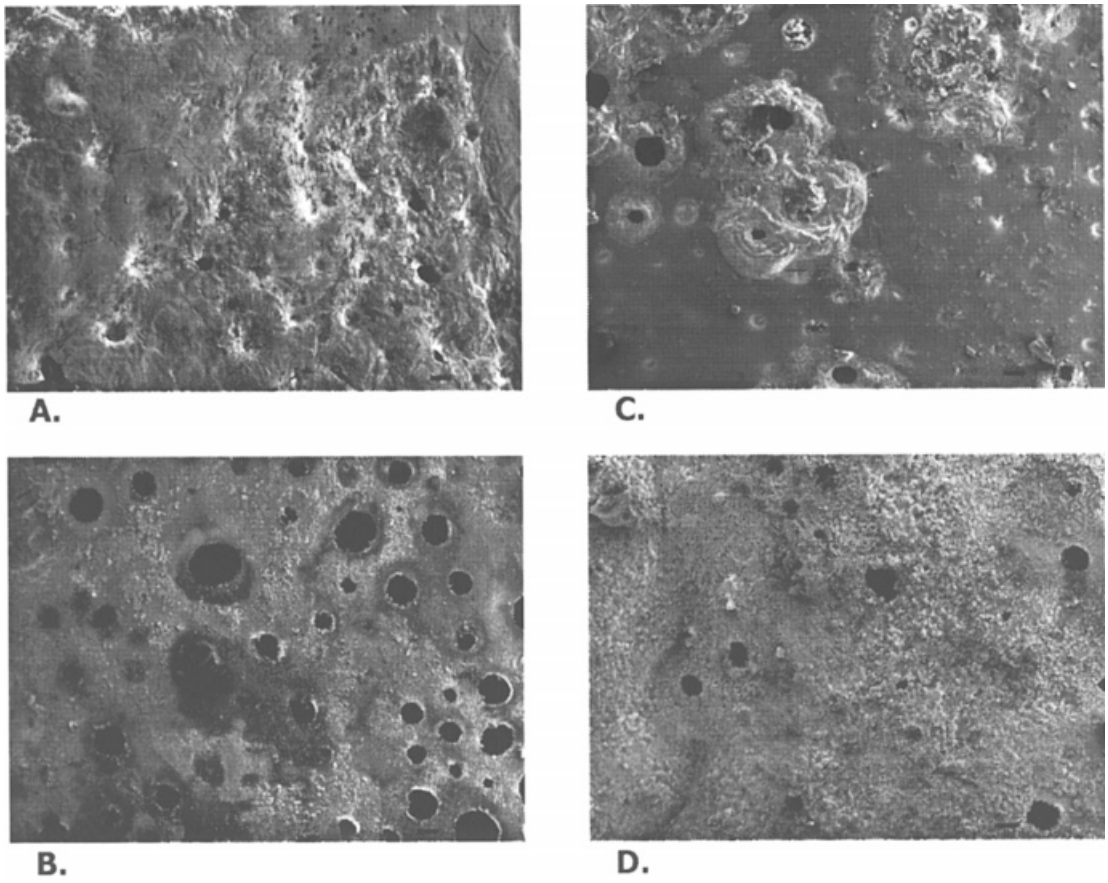

FIGURE 2. Scanning electron micrographs of the surface of poly(acrylamide-co-acrylic acid) superporous hydrogels produced using surfaces modified with hydrophilic agents. The micrographs of the surface of superporous hydrogels produced in glass tubes with unmodified (A), BATS (B), CETS (C), TATS (D) surfaces were taken at a magnification of 50× and the scale bar is 100 μm.

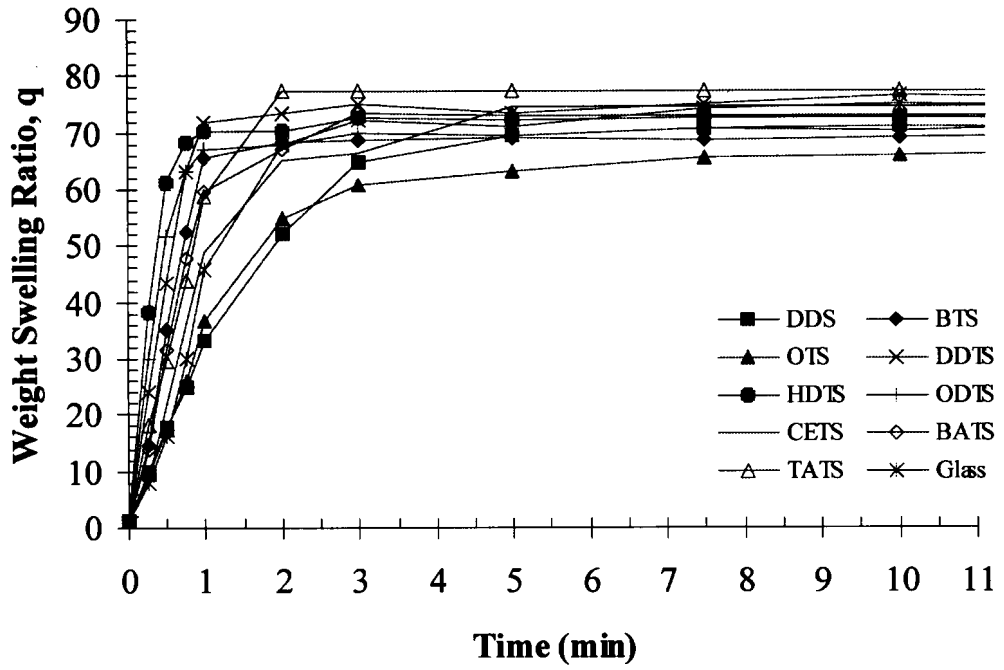

FIGURE 3. Swelling in PBS of poly(acrylamide-co-acrylic acid) superporous hydrogels produced in silanized glass tubes. Each superporous hydrogel is in the cylindrical shape of approximately 3 cm length and 1 cm diameter (n = 3).

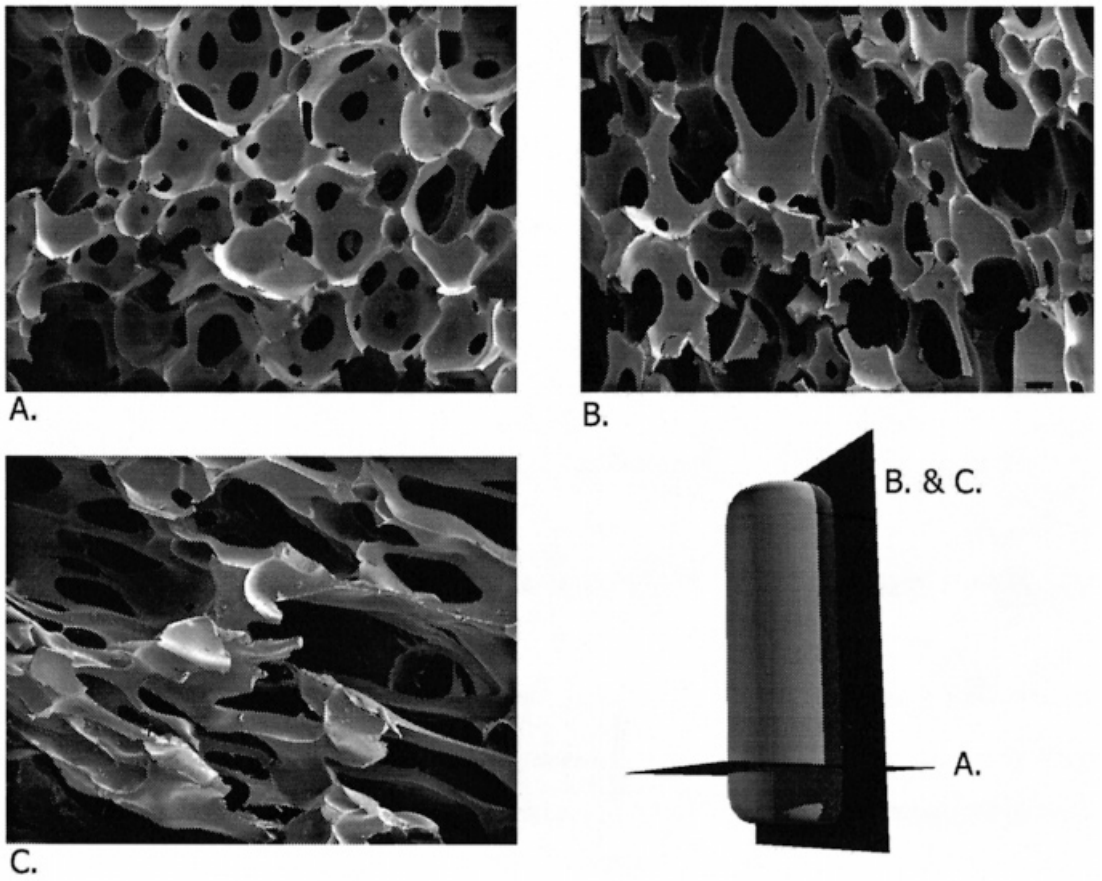

FIGURE 4. Scanning electron micrographs of the internal pore structure of poly(acrylamide-co-acrylic acid) superporous hydrogels. Three images are shown with a cartoon of the direction in which each superporous hydrogel had been cut prior to SEM examination. Image A was cut radially through the superporous hydrogel, while images B and C were cut axially. Image B was taken near the top of the superporous hydrogel while image C was taken near the bottom of the superporous hydrogel. Each image was taken at a magnification of 50× and the scale bar is 100 μm.

TABLE 2. Data Obtained from Mercury Porosimetry for Poly(acrylamide-co-acrylic acid) Superporous Hydrogels Produced in Glass Modified with Silanes

Sample	*Pore diameter (μm)*	*Bulk density (g/ml)*	*Solid density (g/ml)*	*Pore volume (ml/g)*
Non-porous hydrogel	0.01 ±0.00	1.29 ±0.02	1.33 ±0.02	0.03 ±0.00
Unmodified glass	159.81 ±10.57	0.30 ±0.03	1.44 ±0.15	2.65 ±0.19
DDS	145.22 ±11.22	0.36 ±0.04	1.28 ±0.09	2.17 ±0.15
BTS	174.16 ±15.23	0.37 ±0.04	1.38 ±0.10	2.17 ±0.14
OTS	161.93 ±6.98	0.34 ±0.03	1.34 ±0.03	2.18 ±0.14
DDTS	159.75 ±8.01	0.36 ±0.02	1.16 ±0.06	1.95 ±0.07
HDTS	172.12 ±10.58	0.36 ±0.05	1.23 ±0.07	2.04 ±0.26
ODTS	156.97 ±13.35	0.35 ±0.02	1.36 ±0.07	2.19 ±0.10
CETS	157.93 ±11.96	0.30 ±0.03	1.15 ±0.13	2.29 ±0.25
BATS	171.91 ±14.29	0.31 ±0.03	1.26 ±0.10	2.46 ±0.18
TATS	155.13 ±9.75	0.32 ±0.05	1.10 ±0.10	2.34 ±0.34

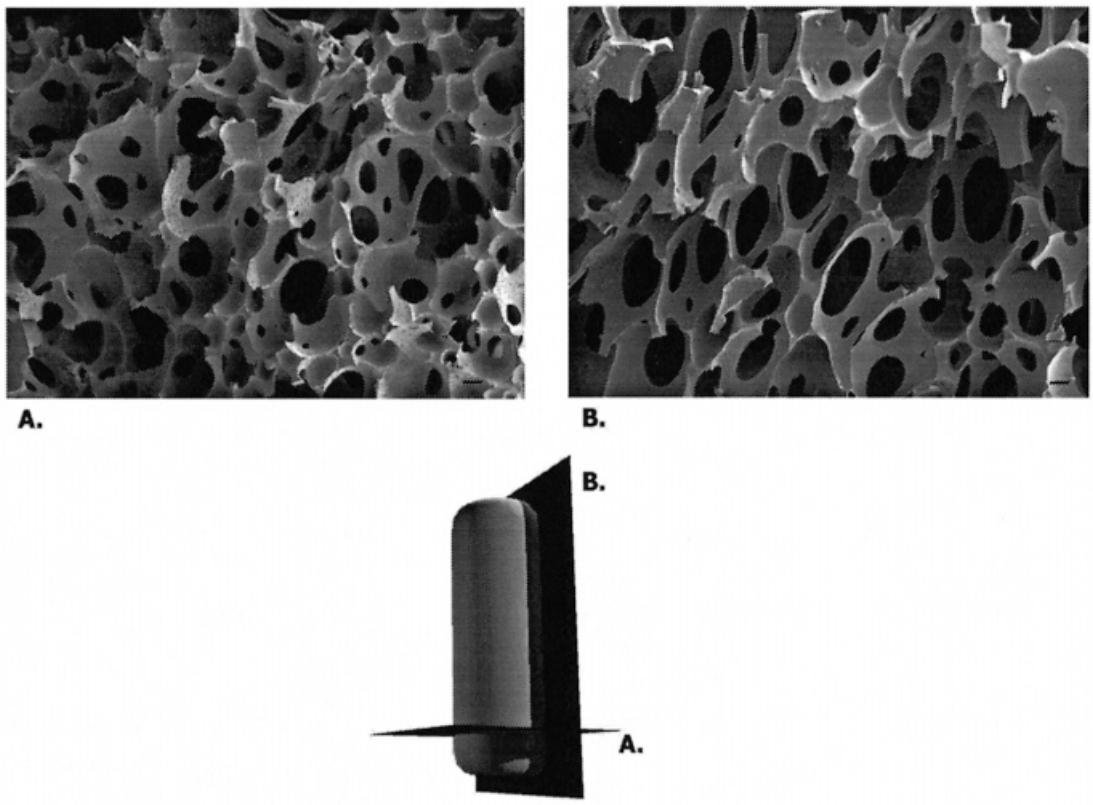

FIGURE 5. Scanning electron micrographs of poly(acrylamide-co-acrylic acid) superporous hydrogels produced in a square mold made of polyethylene. The superporous hydrogel was cut through the short axis (A) and through the long axis (B) so that images equivalent to those of the cylindrical superporous hydrogel were produced. A cartoon of the SPH shows where the cuts were made. The magnification of A and B was 50× and the scale bar is 100 μm.

Internal Pore Morphology

The internal structure of the SPHs was different from the external pore structure. Scanning electron micrographs showed highly connected pores (Fig. 4). The pores were spherical in shape with circular interconnections when the SPHs were cut through the radius of the cylinder (Fig. 4A). This was not true when the SPHs were cut through the axis (Fig. 4B and 4C). This structure was confirmed by taking pictures of SPHs produced in square molds (Fig. 5). When the SPHs were cut through the short axis, spherical pores were found, but when cut through the long axis, elongated pores were found.

Internal Pore Size

Mercury porosimetry measurements indicated that there were no pores present below 8 μm. For this reason, a low-pressure regimen was used for all samples so that accurate examination of large pores could be conducted. The data obtained from porosimetry is presented in Table 2. Pore diameter of each SPH is not statistically different as compared to any sample other than the non-porous hydrogel ($p > 0.10$). The SPHs had low bulk density (0.30 ± 0.03 g/ml). This was expected since there is a large quantity of air inside the SPHs. The density of the solid structure of the SPH was much higher (1.44 ± 0.15). The solid and bulk density of the conventional hydrogel (1.33 ± 0.02) was equivalent to the solid density of the SPH ($p > 0.10$). This also was expected since the SPHs solid structure should be equivalent to the conventional hydrogel. The volume of the pores of the SPHs can be estimated by the intrusion volume from porosimetry. The intrusion volume of the samples is presented as volume intruded per mass of sample. This is to take into account the variability of samples in weight. The volume intruded is also not significantly variable for the SPHs prepared in modified glass culture tubes ($p > 0.10$).

DISCUSSION

In early studies on SPHs, either borosilicate glass or polystyrene culture tubes were used to produce SPHs [4]. No difference in swelling of poly(acrylamide-co-acrylic acid) SPHs was noted between SPHs made in the different molds. It was hypothesized, however, that the properties of the external structure of the SPHs would change by changing the surface of the mold in which the SPH was manufactured. To determine how surface chemistry affected the structure of the pores of the SPH, the surface of glass tubes was modified with silane compounds. Silane chemistry for modification of glass has been utilized extensively in various fields [6–10]. The chemistry is well established and monolayers of modifying agents are expected to be present on the surface.

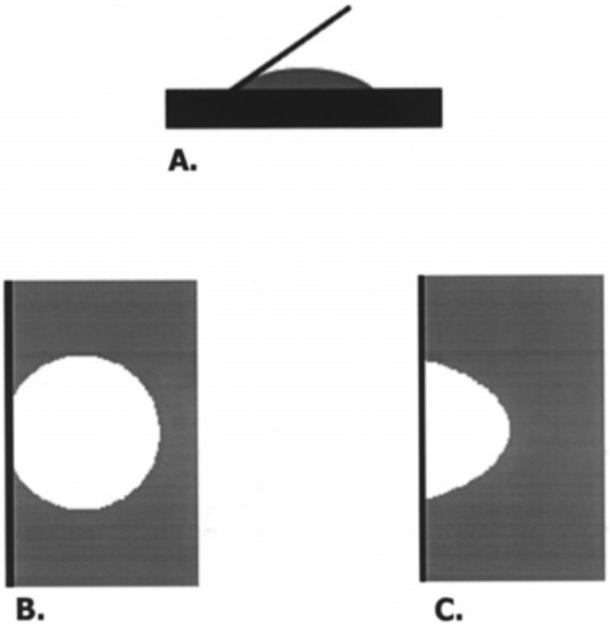

FIGURE 6. Schematic representation of how the surface interaction between the glass and polymerizing solution can affect the pore structure on the surface of the superporous hydrogel. The contact angle between a wetting fluid and a flat plate (A), an air bubble and a wetting fluid (B), and an air bubble and a non-wetting fluid (C).

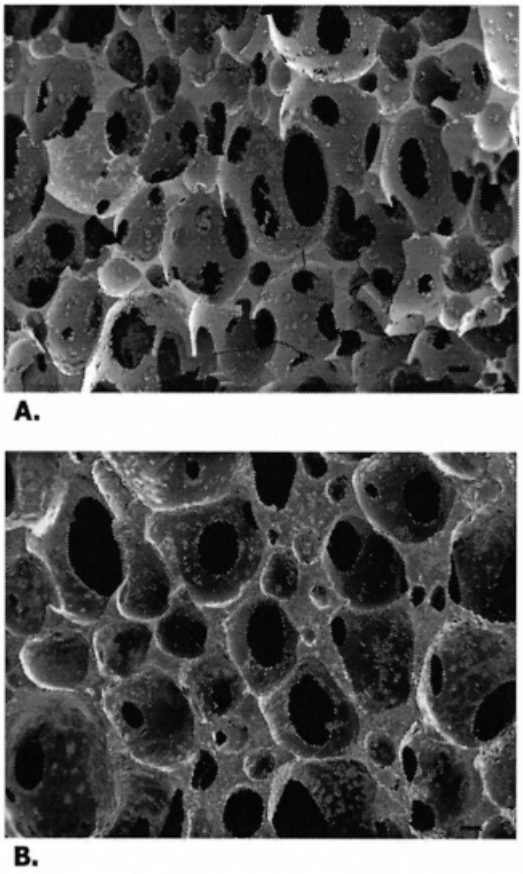

FIGURE 7. Scanning electron micrograph of the internal (A) and external (B) pore structure of a poly(acylamide-co-acrylic acid) superporous hydrogel produced in a HDTS modified glass culture tube. Each image was taken at a magnification of 50× and the scale bar is 100 μm.

The most striking difference between the unmodified glass and a modified surface was that the amino derivatized glass was quite adhesive toward the SPH. It was impossible to remove the SPH from the culture tube without tearing the surface of the SPH. Regardless of the amount of care taken, pieces of the SPH were left on the culture tube. This was most likely due to the carboxylic acid of the acrylic acid and the amide of acrylamide forming hydrogen bonds with the amine on the surface. This resulted in the inability to examine the effect of this surface chemistry on the surface of the SPH. This was not found with any other surface, as expected. The hydrophobic surfaces allowed for easy release of the SPH from the culture tube, which could make manufacturing reproducible SPHs more readily possible.

The air–water–surface contact angle determined the surface structure of the poly(acrylamide-co-acrylic acid) SPHs (Fig. 6). When the surface was hydrophilic ($\theta < 90°$), water wetted the surface and closed off or at least minimized any air bubbles that touch the surface. When the surface was hydrophobic, however, air bubbles that come into contact with the surface were stabilized by the surface tension of water. Once the opening began to be formed, it would enlarge rather than shrink, as was the case for hydrophilic surfaces.

Swelling studies showed that the surface structure of the walls of the SPH did not play a significant role in the swelling of the p(AM-AA) SPHs. This was at first thought to repute our hypothesis that the greater the surface pore content, the greater the ability of the SPH for uptake of solvent. The micrographs in Fig 1 and 2 show that there is not a significant increase in connectivity between the surface pores and the internal pore structure. Comparing the surface porosity with the internal porosity (Fig. 7) indicates that the interconnectivity of the surface pores is much lower than the interconnectivity of the internal pores. The reason for the lack of connectivity of the surface pores could be due to the fact that the pores on the surface are not connected to pores in the direction of the escape of carbon dioxide gas bubbles during foaming. The escape of gas from the SPH during polymerization is thought to be the main factor in promoting interconnectivity of the pores in the SPH. The shape of the pores inside SPHs is predominantly polyhedral; however, the shape of the pores in the direction of gaseous escape from the culture tube is distorted. The carbon dioxide formed during the foaming process can be regarded as escaping the culture tube during the polymerization process. As the gas escapes and the pores form, the gas pressure at the bottom of the culture tube forces gas bubbles through the pore network. As gas bubbles escape through the network, pore connectivity is increased in combination with a directional distortion of the shape of the pores. Since the flow of gas near the surface of

the mold is nearly zero, few interconnections are formed at the surface of the SPH.

To confirm that the interconnections were due to gaseous flow and not shape of the mold, a square mold was also used to produce SPHs. The SPHs were cut across the base (equivalent to radial cut in the cylindrical SPH) and along a side (equivalent to the axial cut). The image of the two portions of the SPH matched exactly to the cylindrical SPHs. The pores are distorted in a similar manner to those of the cylindrical SPHs. The images from the square SPHs has nearly the same pore shape as that of the cylindrically shaped SPHs. Whether the pore shape would remain distorted when a thin layer of SPH is formed has not been examined at this point. Thin sheets of the SPH have been formed with gas escaping along the thin axis and along the long axis. Each of these SPHs swells within a similar amount of time with no visible directionality of the swelling. The thickness of the sheets is similar to the dimensions of the pores, so it is possible that the morphology of the pores would not play a vital role in the swelling of the thin sheets.

Mercury porosimetry was used to determine the pore size of the SPHs. Prior to porosimetry, SEM images and liquid intrusion were used to determine the pore size of the SPHs [14]. From these methods, only a rough estimate of diameters of 100–1000 μm from SEM and 340 μm from liquid intrusion could be calculated. These values were not accurate and were somewhat arbitrary. Liquid intrusion only gave the largest diameter pores and had high variability. Mercury porosimetry is quite well accepted in the determination of the pore size of materials despite the fact that it does not take into account the shape of the pores [5]. Unfortunately, due to high interconnectivity, the directionality of the pores of the SPH could not be confirmed using porosimetry. The fact that the porosities of SPHs produced were not different was surprising since the surfaces were so different between samples prepared in hydrophobic (DDS, BTS, OTS, DDTS, HDTS, and ODTS) and hydrophilic (control, CETS, BATS, and TATS) modified glass culture tubes. This may be due to the fact that the porosity of the surface of the SPHs is small compared to the internal structure, and the surface chemistry does not affect the interior pore shape or size. Surface chemistry only has an effect on the outer portion of the SPH. The remainder of the SPH was unaffected by changes on the surface of the culture tube, not changing the average pore shape or size.

For pharmaceutical applications as a gastric retention device, the SPH may act as a floating gastric retention device prior to swelling due to a low bulk density, aiding in early retention of the device in the fed state [11, 12]. This would create a staged retention for the device that could be more effective and explain why SPHs have been retained in the stomach. As long as liquid was present in the stomach when the SPH was taken, the SPH would float on the surface of the liquid and begin to swell. This has yet to be observed *in vivo*, but has been shown *in vitro* with various fluids. Because of the high connectivity of the pores of the SPH, the SPH could be very effective as a mechanism for gastric retention for drug delivery. Studies are underway to combine the SPH with a rate controlling device to determine if a composite device could be used for drug delivery for extended periods.

ACKNOWLEDGMENT

This study was supported in part by the National Institutes of Health through grant GM 08298. The authors also wish to thank Debra Sherman at the Purdue University Microscopy Center in Agriculture for assistance in the use of a scanning electron microscope. We would also like to thank Hong Wen and Hee-Soo Shin for performing some of the swelling studies.

REFERENCES

1. Wichterle O, Lim D. *Nature* 1960; **185**: 117–118.
2. Chen J, Blevins WE, Park H, Park K. *J. Controlled Rel.* 2000; **64**: 39–51.
3. Hwang S-J, Park H, Park K. *Crit. Rev. Ther. Drug Carrier Sys.* 1998; **15**: 243–284.
4. Chen J, Park H, Park K. *J. Biomed. Mater. Res.* 1999; **44**: 53–62.
5. ASTM. Annual book of ASTM Standards. American Society of Testing and Materials; Philadelphia, PA, (1992); D4284–4292.
6. Witucki GL. *J. Coating Tech.* 1993; **65**: 57–60.
7. Chaimberg M, Cohen Y. *J. Colloid Interf. Sci.* 1990; **134**: 576–579.
8. Arkles B. *Chemtech* 1997; **7**: 766–778.
9. Nishiyama N, Horie K, Asakura T. *J. Appl. Polymer Sci.* 1987; **34**: 1619–1630.
10. Sabata A, Knueppel BA, van Ooij WJ. *J. Testing Eval.* 1995; **23**: 119–125.
11. Bolton S, Desai S. *United States Patent* 4,814,179, 1989.
12. Desai S, Bolton S. *Pharm. Res.* 1993; **10**: 1321–1325.